Published in final edited form as:

J Immunol. 2020 May 01; 204(9): 2439–2446. doi:10.4049/jimmunol.1900963.

Protein kinase C-eta deficiency does not impair antiviral immunity and CD8+ T cell activation

Hsin-Yu Liu[*,+], **Christophe Pedros**[*,+], **Kok-Fai Kong**[*], **Ann J Canonigo-Balancio**[*], **Amnon Altman**[*]

[*] Division of Cell Biology, La Jolla Institute for Immunology, La Jolla, California 92037, USA

Abstract

We reported that protein kinase C-eta (PKCη) forms a novel signaling complex with the checkpoint inhibitory protein CTLA-4 in regulatory T cells (Tregs). This complex is required for the contact-dependent suppressive activity of Tregs, including suppression of anti-tumor immunity. However, the importance of PKCη in protective immunity mediated by T effector (Teff) cells remains unclear. We used mice with germline or conditional, Treg-specific deletion of *Prkch*, the PKCη-encoding gene, to explore $CD8^+$ T cell-dependent antiviral immunity using the lymphocytic choriomeningitis virus Armstrong strain acute infection model, as well as the *in vitro* activation of murine or human $CD8^+$ T cells. Five days following infection, germline $Prkch^{-/-}$ mice displayed enhanced viral clearance compared to control mice. Similarly, *Prkch* Treg-specific conditional knockout (cKO) mice also showed improved viral clearance and displayed enhanced expression of granzyme B (GzmB) and interferon-γ (IFNγ) by both virus-specific and total $CD8^+$ T cells, demonstrating that enhanced viral clearance in germline $Prkch^{-/-}$ mice is caused by PKCη deficiency in Tregs and the resulting functional defect of $Prkch^{-/-}$ Tregs. In addition, purified $Prkch^{-/-}$ mouse $CD8^+$ T cells as well as *PRKCH* knockdown human $CD8^+$ T cells displayed intact, or even enhanced, T cell activation *in vitro* as measured by proliferation and expression of GzmB and IFNγ. Thus, global PKCη deletion does not impair overall $CD8^+$ T cell-mediated immunity, including antiviral immunity, implying that selective pharmacological PKCη inhibition could be safely used *in vivo* to inhibit undesired contact-dependent suppression by Tregs and, thus, enhance tumor-specific and, likely, virus-specific immunity.

Keywords

PKCη; Treg; $CD8^+$ T cell; LCMV

Introduction

Regulatory T cells (Tregs) play a key role in maintaining immune system homeostasis and preventing undesired inflammation and autoimmunity (1, 2). Tregs utilize a variety of

Address correspondence to Dr. Amnon Altman, La Jolla Institute for Immunology, [1] Division of Cell Biology, 9420 Athena Circle, La Jolla, CA 92037. amnon@lji.org.

[+]These authors contributed equally to this work.

Disclosures

The authors have no financial conflicts of interest.

mechanisms to suppress immune responses, including contact-dependent suppression, whereby Tregs engage APCs and inhibit their T cell stimulatory function by, *e.g.*, depleting the stimulatory ligands CD80 and/or CD86 from APCs (3). Our recent work revealed a critical intrinsic role of protein kinase C-eta (PKCη), a member of the novel, Ca^{2+}-independent PKC subfamily, in contact-dependent immune suppression mediated by regulatory T cells (Tregs). CTLA4, a major T cell checkpoint (inhibitory) receptor, which is highly and constitutively expressed on Tregs and is required for their suppressive activity, formed a physical complex with PKCη in Tregs. PKCη-deficient ($Prkch^{-/-}$) Tregs or Tregs expressing a PKCη mutant incapable of associating with CTLA4 displayed impaired contact-dependent suppression, including suppression of tumor immunity (4, 5).

In our previous studies, we have used Tregs purified from $Prkch^{-/-}$ mice, which were adoptively transferred into tumor-bearing recipient mice, demonstrating the important role of Treg-expressed PKCη in mediating the suppression of antitumor immunity (4, 5). Thus, the potential importance of PKCη expression in immune (and other) cells besides Tregs remains unexplored. This question is particularly pertinent when considering the important role of T effector (Teff) cells and, in particular, $CD8^+$ T cells, in mediating protective antiviral and tumor-specific immunity. To address this question and to extend the analysis of the potential importance of PKCη expression in $CD8^+$ T cells, we examined further the *in vitro* polyclonal or antigen-induced activation of PKCη-depleted mouse or human $CD8^+$ T cells, as well as CD8-dependent anti-LCMV immunity in germline or Treg-specific *Prkch* conditional knockout (cKO) mice. Here, we report that germline or Treg-specific PKCη depletion in mouse or human T cells does not impair the activation, proliferation and effector functions of $CD8^+$ T cells *in vitro* and *in vivo* and, in fact, often enhances it significantly. Taken together, these results reveal that selective inhibition of the CTLA4-PKCη signaling pathway is a promising therapeutic strategy to enhance not only anti-tumor immunity but also antiviral immunity without having adverse effects on effector $CD8^+$ T cells.

Materials and Methods

Mice

F*oxp3*-**I**RES-e**G**FP (FIG) B6.Cg-*Foxp3*^{tm2Tch}/J mice from the Jackson Laboratories (JAX #006772) and $Prkch^{-/-}$ mice (now available from the Jackson Laboratory; JAX #018988) have been described (4). To generate mice with a conditional *Prkch* deletion in Tregs, we crossed $Prkch^{fl/fl}$ mice generated by the Knockout Mouse Phenotyping Program (KOMP; [Prkch$^{tm1a(EUCOMM)Hmgu}$]) and bred at The Jackson Laboratory with *Foxp*3-IRES-YFP^{Cre} mice [B6.129(Cg)-Foxp3$^{tm4(YFP/icre)Ayr}$/J; JAX #016959]. All experiments were performed with the approval of the LJI Animal Care Committee and in strict accordance with its guidelines. Eight to 14-week old mice with no gender preference were used.

Lymphocytic Choriomeningitis Virus (LCMV) Models

LCMV Armstrong strain ($LCMV_{Arm}$) was kindly provided by Dr. Shane Crotty (LJI). Mice received 2×10^5 PFU $LCMV_{Arm}$ in a volume of 0.5 ml RPMI-1640 medium by two i.p.

injections of 0.25 ml each to initiate acute infection. All analyses were performed 5 d after infection.

Quantitative RT-PCR (qPCR)

Mouse spleen lysates were subjected to RNA extraction using RNeasy Mini Kit according to the manufacturer's instructions (Qiagen). cDNA was obtained using SuperScript III Reverse Transcriptase (Invitrogen, Carlsbad, CA) with gene-specific primers (NP2-R or GP-R) targeting LCMV nucleoprotein (NP) or envelope glycoprotein (GP) gene, respectively. qPCR assay was performed using iTag Universal SYBR Green Supermix (Bio-Rad, CA). The LCMV-specific primers were designed as described (6). NP2-R (S pos. 2697–2720): 5'-CAGACCTTGGCTTGCTTTACACAG-3'; NP2-F (S pos. 2601–2623): 5'-CAGAAATGTTGATGCTGGACTGC-3'; GP-R (S pos. 970–991): 5'-GCAACTGCTGTGTTCCCGAAAC-3'; GP-F (S pos. 877–901): 5'-CATTCACCTGGACTTTGT CAGACTC-3'. The PCR thermal profile was set as follows: denaturation at 95°C for 30 s; 50 cycles of denaturation at 95°C for 15 s, annealing/extension at 60°C for 30 s; a melting curve at 65–95°C with 0.5°C increment. A standard curve was generated using a 10-fold serial dilution of linearized pCITE-NP (*Eco*RI) or pSG5-GP (*Bam*HI) plasmids, gifts from Dr. Shane Crotty. The corresponding RNA copy numbers were calculated using a previously described formula (7).

Flow cytometry and MHC tetramer staining

Five days post-infection, spleens were collected and weighted. Thereafter, spleens were forced gently through a 70-μm cell strainer using a sterile syringe plunger in 5% FBS/RPMI-1640 medium. The splenocyte suspensions were washed and incubated with 5 ml RBC lysis buffer at RT for 5 min. After quenching the RBC lysis buffer by adding 10% FBS/RPMI-1640 medium, splenocytes were washed and stained with MHC class I H2-D^b tetramers complexed with LCMV $NP_{396–404}$ (NP_{396}: FQPQNGQFI) or $GP_{33–41}$ (GP_{33}: KAVYNFATC) peptides (NIH Tetramer Core Facility) for the detection of epitope-specific $CD8^+$ T cells, and $GP_{66–77}$ (GP_{66}: DIYKGVYQFKSV) peptides for the detection of epitope-specific Treg cells. For antigen-induced cytokine expression, 1×10^6 cells were cultured at 37°C for 5 h in complete medium (10% FBS, 5 mM Hepes, 100 mM non-essential amino acids, 1 mM sodium pyruvate, 100 U/ml each penicillin and streptomycin, 50 μM 2-mercaptoethanol, and 2 mM L-glutamine in RPMI-1640), and stimulated with the LCMV peptides NP_{396}, GP_{33} or GP_{66} (5 μg/ml; AnaSpec), 10 U/ml of recombinant human IL-2, and GolgiStop (1:1,500; BD Biosciences). Surface and intracellular cytokine staining (ICS) were performed using the Cytofix/Cytoperm™ kit (BD Biosciences) at a 1:100 dilution of Abs (Table I) according to the manufacturer's instructions. Samples were acquired on a BD LSR Fortessa flow cytometer and analyzed using the FlowJo software.

CellTrace Violet (CTV) labeling and in vitro mouse $CD8^+$ T cell stimulation

$CD8^+$ T cells were purified from pooled spleen and peripheral lymph node suspensions of WT or *Prkch*$^{-/-}$ mice using a mouse $CD8^+$ T cell isolation kit (MACS, Miltenyi-Biotec, Auburn, CA). To measure cell proliferation, purified $CD8^+$ T cells were stained with 2 μM CTV (Thermo Fisher Scientific, C34557) in pre-warmed PBS under dark incubation at 37°C for 15 min. Staining was stopped by adding FBS at 37°C for 5 min. Cells were washed twice

with 5% FBS/PBS, and seeded at 1×10^5 cells/well in flat-bottom 96-well plates. CTV-labeled $CD8^+$ T cells were stimulated with various concentrations of immobilized anti-CD3 and soluble anti-CD28 mAbs in complete medium for 3 d. For GzmB and IFNγ expression, GolgiStop (Monensin, BD Biosciences) was added for the last 5 h of stimulation. ICS, sample acquisition, and analysis were performed as described above (Table I).

Human $CD8^+$ T cells in vitro expansion and lentiviral transduction

Human blood samples from healthy donors were obtained from the LJI institutional Normal Blood Donor Program (master protocol VD-057). $CD8^+$ T cells were purified from the PBMCs of 4 healthy donors using the EasySep™ Human $CD8^+$ T Cell Enrichment Kit (STEMCELL Technologies) according to the manufacturer's instructions. Five $\times 10^5$ $CD8^+$ T cells were stimulated with anti-CD3 plus anti-CD28-coated microbeads (Invitrogen) at a 1:1 bead-to-cell ratio in 24-well plates in the presence of 30 U/ml IL-2 in ImmunoCult™-XF T Cell Expansion Medium (STEMCELL Technologies) supplemented with 10% human AB serum (Valley biomedical). After 24 h, 500 μl of culture media was removed and replaced with freshly collected supernatants containing lentiviral particles. Supernatants were supplemented with polybrene (Sigma) at a final concentration of 5 μg/ml. Infection with lentiviral particles was performed by centrifugation at $800 \times g$ for 60 min at 37°C. Fresh media containing IL-2 was added to the wells after 24 h, and transduced (GFP^+) $CD8^+$ T cells were purified by cell sorting after 5 d and rested in the absence of anti-human CD3 plus anti-CD28 mAb stimulation but in the presence of IL-2 for 2 additional d. Before restimulation, GFP^+ cells were cultured overnight in the absence of IL-2. PBMC from a different donor were used as a source of APCs. Frozen PBMCs were cultured overnight in media at 37°C in absence of IL-2 or stimulation before use. Fifty x 10^3 transduced GFP^+ CTV labeled $CD8^+$ T cells were stimulated with anti-human CD3 mAb (OKT3, 0.3 μg/ml)-coated 96-well plate flat bottom in presence of 150,000 PBMCs for 4 d *in vitro*. GolgiStop (Monensin, BD biosciences) was added for the last 5 h of stimulation.

Plasmids and lentiviral particles production

Two shRNAs targeting human *PRKCH* (shPRKCH-1 and −2) or an irrelevant control shRNA (shCt) designed by the RNAi Consortium in the pLKO.1 lentiviral vector containing a puromycin selection cassette were obtained from GE Dharmacon. The original pLKO.1-puro vectors were modified to replace the puromycin resistance gene by a fluorescent reporter gene (GFP or Ametrine). HEK293T cells (6×10^5/well in 6-well plate) were transfected with a mixture of the following plasmid DNAs for virion production: pMDGLg/pRRE (Addgene 12251, 1 μg), pRSV-rev (Addgene 12253, 1 μg), pMD2.G (Addgene 12259, 1 μg), pLKO.1-shRNA (2 μg) plasmid DNA.

In vitro Treg suppression assay

Flow cytometry sorted Foxp3 GFP negative T cells (Teff cells) were labeled with 2 μM CTV (Thermo Fisher Scientific, C34557). Labeled Teff cells (3×10^4 cells) and irradiated (3000 rads) T cell-depeleted splenocytes (2×10^5 cells) were co-cultured for 3 d with GFP^+ (WT mice) or YFP^+ (cKO mice) Treg cells ($0.75–6\times 10^4$ cells) in the presence of an anti-mouse CD3 mAb (1μg/ml, clone 2C11). For GzmB expression, GolgiStop (Monensin, BD

Biosciences) was added for the last 5 h of stimulation. ICS, sample acquisition, and analysis were performed as described above.

Bone marrow chimeras

WT and *Prkch*$^{-/-}$ recipient mice were fasted overnight and then lethally irradiated x2 with 500 rads at a 4 h interval. After the second irradiation, 1× 10^7 T cell-depleted bone marrow (BM) cells from donor wild-type (WT) mice were transferred by retroorbital i.v. injection into recipient mice WT or *Prkch*$^{-/-}$ mice. The mice were housed in sterile cages with antibiotic-containing water during −7 d to +14 d. After 8 wk, BM chimeric mice were infected with 2 × 10^5 PFU $LCMV_{Arm}$ for analysis of viral titers as described above.

Statistical analysis

All graphs were plotted and analyzed using GraphPad Prism 7.0. For two group comparisons, the normality of each group was analyzed using a Shapiro-Wilk normality test. Statistical analysis of the normally distributed groups was performed using unpaired *t*-tests. Statistical analysis of non-normally distributed groups was performed using the two-tailed nonparametric Mann-Whitney test. For multiple group comparisons, we applied the two-way ANOVA test with Bonferroni's correction. For human $CD8^+$ T cells assays, analysis was performed using matched one-way ANOVA and paired Student's *t*-test. Data are presented as the mean ± SEM ($n \geq 5$) or ± SD ($n < 5$). n indicates the number of mice in each group.

Results

Enhanced LCMV clearance in germline Prkch$^{-/-}$ mice

To determine the effect of global, germline *Prkch* deletion on antiviral immunity, we infected germline *Prkch*$^{-/-}$ mice or control, WT mice with $LCMV_{Arm}$, and analyzed the response to infection 5 d later by measuring different relevant parameters. Viral load in the spleen, measured by qPCR analysis of mRNA encoding the viral NP or GP revealed a significantly lower virus titer in the *Prkch*$^{-/-}$ mice as compared to the control mice (Fig. 1A), indicating that germline *Prkch* deletion results in enhanced viral clearance. To directly measure LCMV-specific $CD8^+$ T cell responses, we used NP or GP tetramers to identify virus-specific $CD8^+$ T cells that express CD44, a marker of activated/memory T cells. The percentages of NP_{396}^+ (Fig. 1B, top panels) or GP_{33}^+ (Fig. 1B, bottom panels) splenic $CD8^+CD44^+$ T cells were similar in *Prkch*$^{-/-}$ and WT mice. We further analyzed the functional attributes of these cells by stimulating the spleen cells *in vitro* with the corresponding NP or GP peptides and assessing the expression of GzmB or IFNγ, two hallmarks of the effector function of $CD8^+$ CTLs, using intracellular staining (ICS). Again, the percentages of $GzmB^+$ (Fig. 1C, D) or $IFN\gamma^+$ (Fig. 1E, F) Tet^+ $CD8^+$ T cells were similar in *Prkch*$^{-/-}$ and WT mice. We obtained very similar results when we calculated the absolute numbers of $GzmB^+$ or $IFN\gamma^+$ $CD8^+$ T cells (data not shown). These results suggest that the generation and activation of LCMV-specific $CD8^+$ T cells, as well as the protective antiviral response are not compromised in the absence of PKCη.

Enhanced antiviral immunity in Treg-specific Prkch$^{-/-}$ cKO mice

The enhanced viral clearance following germline deletion of *Prkch* (Fig. 1A) could be due to a direct effect on CD8$^+$ Teff cells, an indirect effect on CD8$^+$ T cells resulting from the impaired suppressive activity of the *Prkch*$^{-/-}$ Tregs in these mice or, potentially, the lack of PKCη in other immune or non-immune cells that influence the antiviral response. To begin to address these possibilities and, specifically, examine the contribution of Treg-expressed PKCη, we similarly analyzed the anti-LCMV$_{Arm}$ response in mice, in which *Prkch* has been conditionally and specifically deleted from the Treg compartment. These mice were generated by crossing mice expressing a germline floxed *Prkch* allele (*Prkch*$^{fl/fl}$) with *Foxp3*-IRES-*YFP*^{Cre} mice. Using ICS, we confirmed that, similar to germline *Prkch*$^{-/-}$ mice, these cKO mice lacked expression of PKCη in splenic Foxp3$^+$ Tregs, but not in CD4$^+$Foxp3$^-$ and CD8$^+$ T cells, or in B cells (Fig. S1). We confirmed the resulting decrease in Treg suppressive activity by demonstrating that the *Prkch*$^{-/-}$ Tregs from these mice displayed a significantly reduced ability to suppress the proliferation (Fig. S2A, B) and expression of GzmB (Fig. S2C) in co-cultured CD8$^+$ T cells by comparison with wild-type Tregs (Fig. S2).

Five days following LCMV infection, anti-LCMV$_{Arm}$ viral titers were significantly lower in the cKO mice than in the corresponding control mice (Fig. 2A), despite the fact that the frequency of Tet$^+$ CD8$^+$ T cells was similar in the cKO and control groups (Fig. 2B). Consistent with enhanced antiviral immunity, the Tet$^+$ cells from cKO mice expressed significantly higher levels of GzmB (Fig. 2C, D) and IFNγ (Fig. 2E, F). We further analyzed the effector phase responses of Tregs, and did not observe any differences in the frequencies of both total and LCMV-specific Tregs (Fig. S3A, C), the production of IL-10 and TGFβ (Fig. S3B, D), or the expression of Treg surface markers, *i.e.*, CD25, GITR, and CTLA4 (data not shown) between infected WT and cKO mice. Overall, these results, when compared to the findings in germline *Prkch*$^{-/-}$ mice (Fig. 1), strongly suggest that deletion of PKCη in Tregs is a major contributor to the enhanced viral clearance observed in germline *Prkch*$^{-/-}$ mice, likely reflecting a more potent Teff response in the presence of functionally impaired *Prkch*$^{-/-}$ Tregs.

In order to determine whether *Prkch*$^{-/-}$ non-hematopoietic cells in the germline *Prkch*$^{-/-}$ mice contribute to the observed effects, we also generated BM chimeric mice by transferring BM cells from WT donors into irradiated WT or *Prkch*$^{-/-}$ recipients, followed by LCMV$_{Arm}$ infection. The two groups of recipient mice displayed similar virus titers (Fig. S4), indicating that non-immune cells do not contribute significantly to the enhanced viral clearance we observed in germline *Prkch*$^{-/-}$ mice.

Dispensable role of PKCη in CD8$^+$ T cell activation and proliferation

The above results revealed that GzmB and IFNγ expression by virus-specific CD8$^+$ T cells were not altered following germline *Prkch* deletion (Fig. 1) but were enhanced in the LCMV$_{Arm}$-infected cKO mice (Fig. 2). This difference could reflect some direct effect of PKCη expressed by the CD8$^+$ T cells themselves or, less likely (see Fig. S4), by other cells. To determine whether PKCη is intrinsically required for the activation of CD8$^+$ T cells, we stimulated purified *Prkch*$^{-/-}$ or WT CD8$^+$ T cells with different concentrations of anti-CD3

plus -CD28 mAbs, and measured their proliferation and GzmB or IFNγ expression. We observed no significant difference in the extent of proliferation (Fig. 3A) or the percentage of $CD44^+$ activated/memory T cells (Fig. 3B) between the *Prkch*$^{-/-}$ and WT $CD8^+$ cells. However, analysis of effector function in these cells revealed that *Prkch*$^{-/-}$ $CD8^+$ T cells displayed a tendency toward higher expression of both GzmB (Fig. 3C) and IFNγ (Fig. 3D). These findings suggest a minimal, if any, intrinsic role for PKCη in $CD8^+$ T cell proliferation, but potentially some inhibitory role in the differentiation of these cells into Teff cells. Additionally, we found that *ex vivo Prkch*$^{-/-}$ $CD4^+$ T cells also displayed intact proliferation and production of cytokines in response to *in vitro* anti-CD3- plus -CD28 mAb stimulation (data not shown).

We next extended this analysis to peripheral blood purified human $CD8^+$ T cells, in which PKCη expression was effectively and highly reduced by specific shRNAs (Fig. 4A; 82% −98% knockdown efficiency). The cells were stimulated *in vitro* an anti-CD3 mAb plus APCs prior to assessing their proliferation and effector functions. Although *PRKCH* knockdown appeared to delay the proliferation of $CD8^+$ T cells from donor #2 (but not of other donors), as reflected by the CTV dilution histograms (Fig. 4B), further analysis of the proliferation index (Fig. 4C) and the % of divided cells (Fig. 4D) revealed that *PRKCH* knockdown had no inhibitory effect on the overall proliferation of cells from all 4 donors. However, we observed a significant increase in the frequencies of $GzmB^+$ and $IFN\gamma^+$ cells from 3/4 donors following *PRKCH* knockdown (Fig. 4E, F). In conclusion, PKCη deficiency in both murine and human $CD8^+$ T cells did not impair their proliferation, and seemed to enhance their effector function measured by GzmB and IFNγ expression.

Discussion

Our previous work has uncovered a novel Treg-intrinsic signaling pathway, which consists of a physical complex between CTLA-4, a major T cell inhibitory receptor, which is constitutively expressed on Tregs and is required for their suppressive activity (9), and the PKC family member PKCη (4, 5). This signaling pathway plays an obligatory role in contact-dependent suppression mediated by Tregs, as judged from analysis of Tregs that were genetically deficient for PKCη or expressed a PKCη mutant incapable of associating with CTLA-4. We found that this signaling complex controlled the Treg-mediated depletion of the DC costimulatory ligand CD86 (5) via the previously established process of transendocytosis (3). Furthermore, Tregs lacking PKCη displayed a severe defect in their ability to suppress tumor immunity (but not experimental autoimmune colitis), which was reflected by reduced tumor growth and increased expansion and effector function of intratumoral $CD8^+$ T cells (4, 5). Our findings thus raised the possibility that pharmacological inhibition of PKCη or disruption of its interaction with CTLA-4 could have clinical implications in the arena of cancer immunotherapy by inactivating Tregs and, thus, enhance tumor-specific immunity in cancer patients.

Given these findings, we reasoned it would be important to determine whether PKCη is required for the activation and effector function of $CD8^+$ T cells, which play a well-established and important role as cytotoxic effector cells for the killing of tumor cells (10) and virus-infected cells (11). Here, we addressed the importance of PKCη in $CD8^+$ by

studying CD8-dependent anti-LCMV immunity in *Prkch*$^{-/-}$ mice and by analyzing the *in vitro* activation of PKCη-depleted mouse and human CD8^{+} T cells. We found that mice with either germline or Treg-specific *Prkch* deletion displayed enhanced acute clearance of $LCMV_{Arm}$ as judged by qPCR analysis of two major viral proteins, NP and GP. This increase likely reflects the greatly impaired ability of the *Prkch*$^{-/-}$ Tregs in these mice to suppress the activation and effector function of virus-specific CD8^{+} T cells, resulting in more efficient activation and expansion of these Teff cells. Furthermore, global or Treg-specific lack of PKCη did not lead to any decrease in the proportion of NP or GP Tet^{+} memory/activated (CD44^{+}) CD8^{+} T cells, nor did it impair the expression of effector molecules, *i.e.*, GzmB and IFNγ, in LCMV Tet^{+} or total CD8^{+} T cells from the infected mice. Rather, Treg-specific, but not germline, *Prkch* deletion led to a significant increase in the proportion of Tet^{+} or total CD8^{+} T cells that expressed GzmB or IFNγ. The reasons for this difference in the effector function of CD8^{+} T cells derived from germline *versus* Treg-specific *Prkch* cKO mice are not clear, but could reflect effects of PKCη deletion in some host hematopoietic cells besides Tregs, which modulate the antiviral Teff response. Our bone marrow transfer experiment demonstrates, however, that non-immune cells did not contribute significantly to these differences since the infection of chimeric mice that received WT or *Prkch*$^{-/-}$ BM cells, but otherwise contained WT or *Prkch*$^{-/-}$ non-immune cells, resulted in similar virus titers. Overall, the similarity in antiviral immunity between germline or Treg-specific *Prkch* cKO mice indicates that deletion of PKCη in the Treg compartment, rather than in other host cells, is the major, if not exclusive, driver of the enhanced viral clearance and CD8^{+} T cell effector function.

Our analysis of purified CD8^{+} T cells from germline *Prkch*$^{-/-}$ or Treg-specific *Prkch*$^{-/-}$ cKO mice revealed that these CD8^{+} T cells proliferated to the same extent as WT CD8^{+} T cells in response to anti-CD3 plus -CD28 costimulation. We similarly found intact proliferation of *PRKCH* knockdown human CD8^{+} T cells, leading us to conclude that CD8-intrinsic PKCη expression is not required for their TCR-induced *in vitro* proliferation. With regard to the expression of effector molecules, we found that CD8^{+} T cells from Treg-specific cKO mice displayed a statistically significant increase in IFNγ and GzmB expression. Such an increase was not found, however, in CD8^{+} T cells from germline *Prkch*$^{-/-}$ mice, perhaps reflecting indirect *in vivo* effects of PKCη deletion in some host immune cells on the CD8^{+} T cells, which alter the *in vitro* differentiation of the isolated CD8^{+} T cells into Teff cells (12). In the case of human CD8^{+} T cells, in which *PRKCH* was knocked down in a highly effective manner, we also observed intact *in vitro* proliferation and GzmB or IFNγ expression, although there was some tendency toward increased expression of these molecules, which, however, for the most part did not reach statistical significance. From these results we conclude that, overall, PKCη expression in CD8^{+} T cells, both mouse and human, is dispensable for their TCR-mediated activation and effector function.

Previous analysis of germline *Prkch*$^{-/-}$ mice revealed that PKCη is dispensable for thymocyte development. However, peripheral CD8^{+} T cells from these mice displayed a moderately impaired *in vitro* proliferation induced by an anti-CD3 mAb or by specific antigen (ovalbumin) presented by APCs, despite a normal response to phorbol ester plus ionomycin stimulation (12). Some TCR-induced signaling events, including Ca^{2+} influx and activation of NF-κB, were also reduced in anti-CD3 mAb-stimulated *Prkch*$^{-/-}$ CD8^{+} T cells,

and the *in vivo* homeostatic proliferation of these cells was also impaired (12). We, however, did not observe any defects in the *in vitro* proliferation and effector functions of *Prkch*$^{-/-}$ CD8^{+} T cells. This difference could result from different stimulation conditions. For example, in contrast to the previous study, in which the *Prkch*$^{-/-}$ CD8^{+} T cells were stimulated *in vitro* with anti-CD3 alone (12), we stimulated the cells with anti-CD3 plus -CD28 mAbs and, thus, the moderately reduced proliferation reported earlier (12) could reflect the lack of a CD28 costimulatory signal.

Our conclusion that the lack of PKCη expression in CD8^{+} T cells does not impair effective antiviral immunity *in vivo* is indirect because it is based on the similarity in CD8-dependent anti-LCMV responses between germline *Prkch*$^{-/-}$ mice, whose CD8^{+} T cell do not express PKCη, and Treg-specific *Prkch* cKO mice, in which the CD8^{+} T cells do express PKCη. Nevertheless, this conclusion is directly supported by our experiments, in which we analyzed the *in vitro* activation and effector function of purified mouse *Prkch*$^{-/-}$ or human *PRKCH* knocked-down CD8^{+} T cells. We are currently in the process of generating mice that specifically lack PKCη expression in CD8^{+} T cells, which will allow us to directly explore the importance of CD8^{+} T cell PKCη expression in antiviral and antitumor immunity *in vivo*.

In summary, our findings imply that pharmacological (or other) inhibition of PKCη function or its interaction with CTLA-4 in clinical contexts will not have any adverse effects on desired immune responses that are mediated by CD8^{+} Teff cells, such as antiviral immunity or tumor-specific immunity. The potential clinical safety of Treg-inactivating PKCη inhibition in cancer patients is also supported by our unpublished observation that germline *Prkch*$^{-/-}$ mice did not display any overt pathology when followed up to an advanced age of at least 12 months (4). This is in sharp contrast to *Ctla4*$^{-/-}$ mice, which display an early lethal lymphoproliferative/inflammatory disease (13, 14), or cancer patients that are treated with checkpoint blockade anti-CTLA-4 Abs, who also develop toxic autoimmune and inflammatory manifestations referred to as immune-related adverse events (15, 16). Indeed, we found that *Prkch*$^{-/-}$ Tregs, despite their impaired ability to suppress antitumor immunity, retain the ability to inhibit experimental autoimmune colitis (4). Hence, the development of approaches aimed at blocking the function of PKCη in order to promote antitumor immunity in cancer patients is likely an attractive strategy with potentially minimal toxic side effects to be further explored.

Supplementary Material

Refer to Web version on PubMed Central for supplementary material.

Acknowledgments

We thank Dr. Shane Crotty (LJI) for providing the LCMV$_{Arm}$ strain, Dr. Simon Belanger for helpful advice in setting up the LCMV mouse model, and the staffs of the LJI animal and flow cytometry facilities for excellent support.

This is publication number 3328 from the La Jolla Institute for Immunology. This work was supported by NIH grant CA233862.

Abbreviations used in this article

BM	bone marrow
cKO	conditional knockout
CTV	CellTrace Violet™
GP	envelope glycoprotein
GzmB	granzyme B
IFNγ	interferon-γ
LCMV	lymphocytic choriomeningitis virus
NP	nucleoprotein
Teff	effector T cell
TNFα	tumor necrosis factor-α
Treg	regulatory T cell

References

1. Maloy KJ, and Powrie F. 2001 Regulatory T cells in the control of immune pathology. Nat Immunol 2: 816–822. [PubMed: 11526392]
2. Sakaguchi S, Ono M, Setoguchi R, Yagi H, Hori S, Fehervari Z, Shimizu J, Takahashi T, and Nomura T. 2006 Foxp3+ CD25+ CD4+ natural regulatory T cells in dominant self-tolerance and autoimmune disease. Immunol Rev 212: 8–27. [PubMed: 16903903]
3. Qureshi OS, Zheng Y, Nakamura K, Attridge K, Manzotti C, Schmidt EM, Baker J, Jeffery LE, Kaur S, Briggs Z, Hou TZ, Futter CE, Anderson G, Walker LS, and Sansom DM. 2011 Trans-endocytosis of CD80 and CD86: a molecular basis for the cell-extrinsic function of CTLA-4. Science 332: 600–603. [PubMed: 21474713]
4. Kong KF, Fu G, Zhang Y, Yokosuka T, Casas J, Canonigo-Balancio AJ, Becart S, Kim G, Yates JR 3rd, Kronenberg M, Saito T, Gascoigne NR, and Altman A. 2014 Protein kinase C-eta controls CTLA-4-mediated regulatory T cell function. Nat Immunol 15: 465–472. [PubMed: 24705298]
5. Pedros C, Canonigo-Balancio AJ, Kong KF, and Altman A. 2017 Requirement of Treg-intrinsic CTLA4/PKCeta signaling pathway for suppressing tumor immunity. JCI Insight 2.
6. McCausland MM, and Crotty S. 2008 Quantitative PCR technique for detecting lymphocytic choriomeningitis virus in vivo. J Virol Methods 147: 167–176. [PubMed: 17920702]
7. Lee C, Kim J, Shin SG, and Hwang S. 2006 Absolute and relative QPCR quantification of plasmid copy number in Escherichia coli. J Biotechnol 123: 273–280. [PubMed: 16388869]
8. Dempsey EC, Newton AC, Mochly-Rosen D, Fields AP, Reyland ME, Insel PA, and Messing RO. 2000 Protein kinase C isozymes and the regulation of diverse cell responses. Am J Physiol Lung Cell Mol Physiol 279: L429–438. [PubMed: 10956616]
9. Wing K, Onishi Y, Prieto-Martin P, Yamaguchi T, Miyara M, Fehervari Z, Nomura T, and Sakaguchi S. 2008 CTLA-4 control over Foxp3+ regulatory T cell function. Science 322: 271–275. [PubMed: 18845758]
10. Restifo NP, Dudley ME, and Rosenberg SA. 2012 Adoptive immunotherapy for cancer: harnessing the T cell response. Nat Rev Immunol 12: 269–281. [PubMed: 22437939]
11. Yap KL, Ada GL, and McKenzie IF. 1978 Transfer of specific cytotoxic T lymphocytes protects mice inoculated with influenza virus. Nature 273: 238–239. [PubMed: 306072]

12. Fu G, Hu J, Niederberger-Magnenat N, Rybakin V, Casas J, Yachi PP, Feldstein S, Ma B, Hoerter JA, Ampudia J, Rigaud S, Lambolez F, Gavin AL, Sauer K, Cheroutre H, and Gascoigne NR. 2011 Protein kinase C eta is required for T cell activation and homeostatic proliferation. Sci Signal 4: ra84. [PubMed: 22155788]

13. Tivol EA, Borriello F, Schweitzer AN, Lynch WP, Bluestone JA, and Sharpe AH. 1995 Loss of CTLA-4 leads to massive lymphoproliferation and fatal multiorgan tissue destruction, revealing a critical negative regulatory role of CTLA-4. Immunity 3: 541–547. [PubMed: 7584144]

14. Waterhouse P, Penninger JM, Timms E, Wakeham A, Shahinian A, Lee KP, Thompson CB, Griesser H, and Mak TW. 1995 Lymphoproliferative disorders with early lethality in mice deficient in Ctla-4. Science 270: 985–988. [PubMed: 7481803]

15. Connolly C, Bambhania K, and Naidoo J. 2019 Immune-Related Adverse Events: A Case-Based Approach. Front Oncol 9: 530. [PubMed: 31293970]

16. Young A, Quandt Z, and Bluestone JA. 2018 The Balancing Act between Cancer Immunity and Autoimmunity in Response to Immunotherapy. Cancer Immunol Res 6: 1445–1452. [PubMed: 30510057]

Key points

- PKCη deletion does not impair immunity against LCMV infection
- PKCη-depleted murine or human $CD8^+$ display intact activation and effector functions

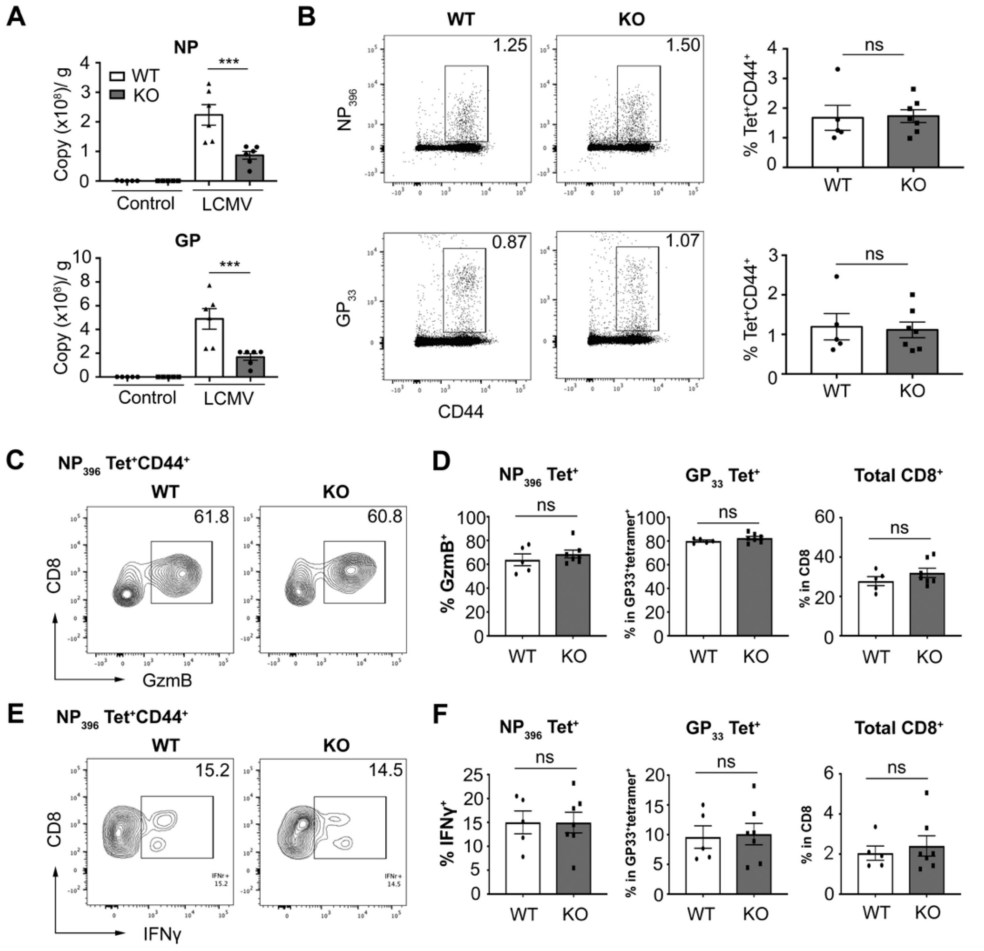

FIGURE 1.

Enhanced viral clearance and intact effector function in germline *Prkch*$^{-/-}$ mice. WT and *Prkch*$^{-/-}$ (KO) mice were infected i.p. with 2×10^5 PFU $LCMV_{Arm}$. **(A)** LCMV-NP and LCMV-GP RNA copy numbers were detected by qPCR in the spleens of WT and KO mice following i.p. infection with LCMV for 5 d. Dots indicate individual mice. WT, n = 5; KO, n = 5. LCMV-infected WT, n = 6; LCMV-infected KO, n = 6. (**B**, **C**-**F**) Leukocytes were isolated from the spleens of infected mice, followed by surface staining with LCMV-NP_{396} (top panels) and LCMV-GP_{33} (bottom panels) tetramers (Tet) in a representative WT or KO mouse (left and middle panels), or in all mice in each group (right panel) (**B**), or *in vitro* restimulation for 5 h with LCMV NP_{396} and GP_{33} peptides in the presence of GolgiStop and human IL-2 (**C**-**F**). **(C**, **E)** Flow cytometry plots of $GzmB^+$ (**C**) or IFNγ^+ cells (**E**) in NP_{396} $Tet^+CD44^+CD8^+$ T cells from a representative mouse. **(D**, **F)** The frequency of $GzmB^+$ (**D**) or IFNγ^+ (**F**) cells in NP_{396} $Tet^+CD44^+CD8^+$ (left), GP_{33} $Tet^+CD44^+CD8^+$ T cells (middle), and total $CD8^+$ T cells (right) from the LCMV-infected mice. Numbers in (**B**, **C**, **E**) represent the % of cells in the boxed areas. Data shown are representative of 3 independent experiments. Data are presented as mean ± SEM, and were analyzed by two-way ANOVA (**A**) or unpaired Student's *t*-test (**B**, **D**, **F**). ***$P < 0.001$; ns, non-significant.

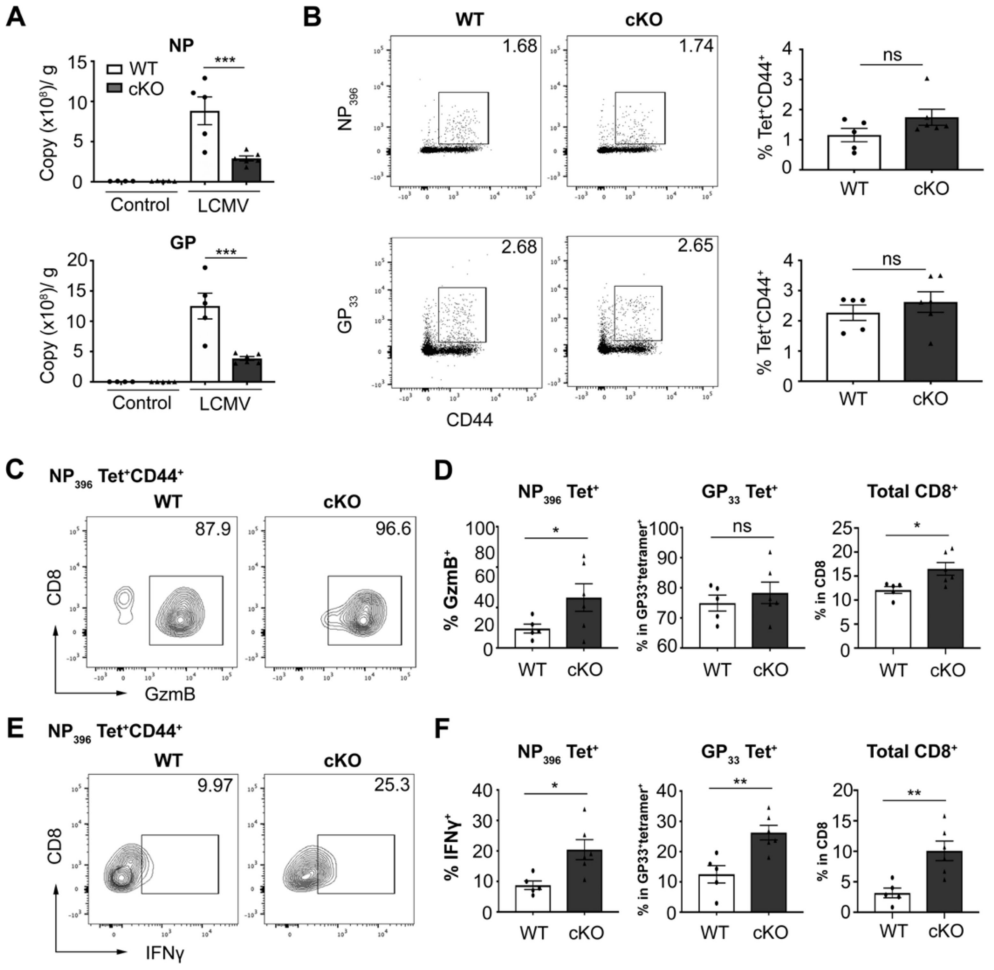

FIGURE 2.

Enhanced viral clearance and effector function in Treg-specific *Prkch*$^{fl/fl}$ x *Foxp3*^{Cre} (cKO) mice. WT and cKO mice were infected i.p. with 2×10^5 PFU $LCMV_{Arm}$ for 5 d. **(A)** LCMV-NP RNA and LCMV-GP RNA copy numbers were detected as in Fig. 1A. Dots indicate individual mice. WT, n = 4; cKO, n = 5; LCMV-infected WT, n = 5; LCMV-infected cKO, n = 6. (**B**, **C**-**F**) Leukocytes were isolated from the spleens of infected mice, and analyzed as in Fig. 1B, **C**-**F**. Numbers in (**B**, **C**, **E**) represent the % of cells in the boxed areas. Data shown are representative of 2 independent experiments. Data are presented as mean ± SEM, and were analyzed as in Fig. 1. ***$P < 0.001$; **$P < 0.01$; *$P < 0.05$. ns, non-significant

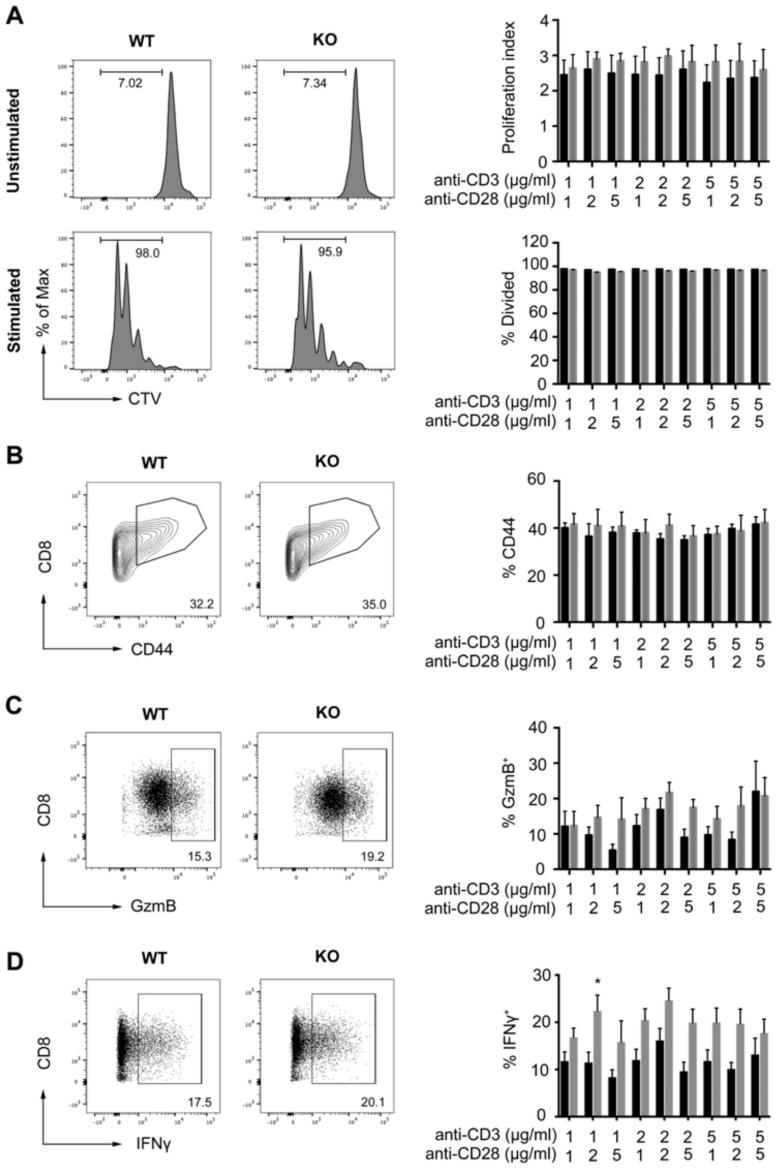

FIGURE 3.

In vitro activation of *Prkch*$^{-/-}$ CD8$^+$ T cells. Purified pooled splenic plus peripheral lymph node CD8$^+$ T cells from WT or KO mice were left unstimulated or stimulated with the indicated concentrations of anti-CD3 plus anti-CD28 mAbs for 3 d. (**A**) Left and middle panels, Representative CTV dilution profiles of unstimulated cells (top) or cells stimulated with anti-CD3 plus anti-CD28 mAbs (2 μg/ml each; bottom). The % of divided T cells is indicated by the horizontal brackets. Right panel, quantification of the proliferation index (top) and % of divided (bottom) CD8$^+$ T cells. **(B)** Frequency of CD8$^+$CD44$^+$ T cells. (**C**, **D**) The frequencies of GzmB$^+$ (**C**) or IFNγ^+ (**D**) CD8$^+$ T cells. Numbers in (**B**-**D**; left panels) represent the % of cells in the bracketed areas. Data were analyzed by two-way ANOVA, and are presented as mean ± SEM. *$P < 0.05$. Pooled data are from 2 independent experiments. WT mice, n = 7; KO mice, n = 7.

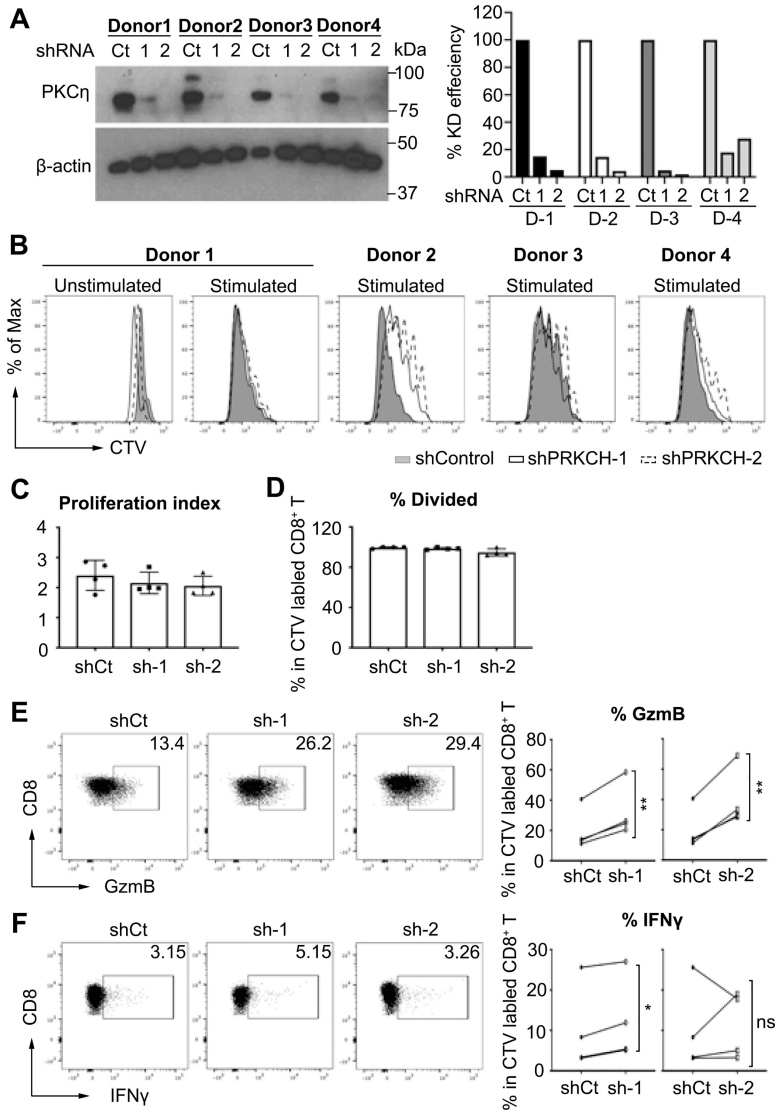

FIGURE 4.

Effect of *PRKCH* knockdown on the activation of human CD8$^+$ T cells. Human CD8$^+$ T cells were purified from the PBMCs of 4 healthy donors, and lentivirally transduced with irrelevant control shRNA (shCt) or two *PRKCH*-targeting shRNA (sh-1 and sh-2). **(A)** Anti-PKCη immunoblot (top left) and densitometric quantitation (right) showing the efficiency of *PRKCH* knockdown (KD) in CD8$^+$ T cells (top panel). Beta-actin was used as an internal control (bottom left). **(B-D)** Proliferation of transduced CD8$^+$ T cells restimulated *in vitro* for 4 d with anti-CD3 mAb (0.3μg/ml) plus APCs showing the CTV dilution profiles (**B**), proliferation index and **(C)**, and % divided **(D)** CD8$^+$ T cells from individual donors. Each dot in (**C**) and(**D**) represents an individual donor. **(E**, **F)** Frequencies of GzmB$^+$ (**E**) and IFNγ$^+$ **(F)** cells among divided CD8$^+$ T cells. Data were analyzed by matched one-way ANOVA (**C**, **D**) or paired Student's *t*-test (**E**, **F**) and are presented as mean ± SD. Data shown are representative of 2 independent experiments. **P* < 0.05; ***P* < 0.01s2

Table I

Antibody	Clone	Fluorophore	Source	Dilution
Anti-mCD28	37.51	Unconjugated	BioLegend	-
Anti-mCD3ε	145–2C11	Unconjugated	“	-
		PerCP-Cy5.5	“	1:200
Anti-mCD8	53–6.7	Alexa Fluor 700	“	1:200
		BV570	“	1:200
		Alexa Fluor 647	“	1:200
Anti-mCD4	GK1.5	APC-Cy7	“	1:200
		AF700	“	1:200
		PerCP/Cy5.5	“	1:300
Anti-mCD19	6D5	BV785	“	1:100
Anti-mIFNg	XMG1.2	PE-Cy7	“	1:100
Anti-mIL10	JES5–16E3	PE-Cy7	“	1:100
Anti-mTGFb1	TW7–16B4	PE	“	1:100
Anti-m/hCD44	IM7	BV570	“	1:100
		BV711	“	1:300
Anti-m/hGzmB	GB11	Pacific Blue	“	1:100
		Alexa Fluor 647	“	1:100
	QA16A02	PE	“	1:200
Anti-hCD4	RM4–5	PE-Cy7	“	1:200
Anti-hCD8	SK1	PerCP	“	1:200
Anti-hIFNg	4S.B3	PE	“	1:200
Anti-hCD3e	OKT3	unconjugated	“	-
Anti-mFoxp3	FJK-16s	FITC	ThermoFisher Scientific	1:100
Anti-rabbit IgG		Alexa Fluor 647	“	1:200
Anti-mPKCh	ab179524	RabMab EPR18513	Abcam	1:500